Journal of Engineering and Technology for Industrial Applications

ITEGAM-JETIA

Manaus, v.11n.55, p. 73-85. September/October, 2025.
DOI: https://doi.org/10.5935/jetia.v11i55.1892

ISSN ONLINE: 2447-0228

RESEARCH ARTICLE OPEN ACCESS

PARAMETERS ESTIMATION OF THREE-PHASE INDUCTION MOTOR USING THE PARAMETER ESTIMATOR APP

Fares Bettahar[1], Sabrina Abdeddaim[2], Omar Charrouf[3], Achour Betka[4] Michael Short[5],Laid Guerrida[6] and Belahcene taha lemdjed[7]

[1, 2, 3, 4]Electrical Engineering Department, LGEB Laboratory, University of Biskra, Algeria.
[5]School of Computing Engineering and Digital Technologies ,Teesside University.
[6]Applied Automation and Industrial Diagnostics Laboratory ,University of Djelfa, Algeria.
[7]Laboratory of Identification, Control, Command, and Communication.,University of Biskra, Algeria

[1]https://orcid.org/0009-0005-0520-092X.[2]https://orcid.org/0009-0006-0812-1554.[3]http://orcid.org/0000-0003-4254-464X
[4]https://orcid.org/0000-0002-7116-4649.[5]https://orcid.org/0000-0001-6290-4396.[6]https://orcid.org/0009-0003-0782-3798
[7]https://orcid.org/0009-0006-9390-937X

Email: fares.bettahar@univ-biskra.dz, sabrina.abdeddaim@univ-biskra.dz, omar.charrouf@univ-biskra.dz
a.betka@univ-biskra.dz, m.short@tees.ac.uk, laid.guerrida@univ-djelfa.dz , Taha.belahcene@univ-biskra.dz

ARTICLE INFO

Article History
Received: April 18, 2025
Revised: May 20, 2025
Accepted: September 15, 2025
Published: September 30, 2025

Keywords:
Induction Motor
Motor Speed
Stator Voltage
Stator Current
Parameter Estimator App

ABSTRACT

Induction motors are among the most widely used electric motors worldwide, valued for their efficiency, robustness, and low maintenance. However, optimizing their performance requires accurate knowledge of electrical and mechanical parameters, which are nonlinear and subject to variation due to aging and operational wear. This study presents a parameter estimation technique using MATLAB's Parameter Estimator app to determine key parameters, including stator and rotor resistances, leakage and magnetizing inductances, moment of inertia, and friction coefficient. The approach relies on experimentally measured inputs such as stator voltage, current, and motor speed, which are applied to a state-space induction motor model in MATLAB. The simulation results are compared with experimental data, specifically motor speed, d-axis current (ids) and q-axis current (iqs). The app iteratively refines the estimated parameters by minimizing the error between simulated and experimental responses. Validation using experimental data from a Siemens induction motor confirms the method's accuracy and reliability, providing a robust framework for precise parameter estimation and enhanced motor control.

I. INTRODUCTION

Nikola Tesla designed the induction motor in 1892, leveraging the advantages of the alternating current (AC) supply system as an alternative to direct current (DC) motors [1]. Since then, induction motors (IMs) have become one of the most widely used electric machines in industrial applications due to their simple structure, ease of operation, low maintenance requirements, and cost-effectiveness [2]. Their robust construction and minimal upkeep make them a preferred choice for various applications, ranging from household appliances to heavy industrial machinery. Given their widespread use, understanding their performance characteristics is crucial for optimizing their operation and ensuring energy efficiency [3].

Induction motors rely on advanced control techniques such as field-oriented control (FOC) [4], direct torque control (DTC) [5], and model predictive control (MPC) [6] to achieve high dynamic performance. However, the effectiveness of these control methods is highly dependent on accurate motor parameter estimation. In FOC, rotor flux orientation is determined by the slip frequency, which is directly influenced by rotor resistance and inductance. Parameter mismatches can lead to poor decoupling of torque and flux, degrading control performance [7]. Similarly, DTC, which directly regulates torque and flux without a modulator, is highly sensitive to variations in stator resistance and inductance. Any inaccuracies can cause flux estimation errors, excessive torque ripple, and degraded steady-state

performance. Likewise, MPC, an optimization-based control strategy, relies on a predictive model to determine the optimal switching states. Parameter uncertainties in resistances, inductances, and mechanical properties can result in inaccurate state predictions, leading to reduced efficiency and compromised transient response [8]. Consequently, precise parameter estimation is essential for ensuring accurate control, minimizing losses, and enhancing the overall reliability of induction motor drives.

The impact of parameter mismatches on control performance has been widely studied in the literature [9,10], as variations in rotor resistance (Rr), stator resistance (Rs), rotor inductance (Lr), and stator inductance (Ls) can reach up to 100% of their nominal values due to temperature fluctuations, aging, and operational wear [11]. These uncertainties are particularly critical in control schemes, where inaccurate motor parameters amplify estimation errors, leading to degraded speed, torque, and flux regulation [12]. Such discrepancies not only reduce control accuracy but also impair overall system efficiency.

The adverse effects of parameter uncertainty are even more pronounced in sensor less control schemes, where the absence of direct mechanical sensors necessitates reliance on parameter-dependent estimation techniques [13]. Precise estimation of rotor position, speed, and flux hinges on accurate knowledge of motor parameters. For instance, errors in Rr or Lr directly affect back-EMF calculations in model-based observers (e.g., sliding-mode observers), leading to biased speed estimates, oscillatory torque responses, and instability [14]. Similarly, mismatches in Ls or Rs distort flux-linkage and torque-current mappings, undermining FOC decoupling and triggering cross-talk between torque and flux [15], [16].

Traditionally, motor nameplates do not provide essential parameters such as stator resistance or leakage inductance, necessitating direct measurement [17]. Common methods for parameter identification include short-circuit and no-load tests [18]. However, these approaches are often impractical due to operational constraints or the unavailability of specialized equipment [19]. Consequently, alternative parameter identification methods have been developed, including offline and online estimation techniques, adaptive algorithms, and observer-based approaches, which allow for more accurate and real-time estimation without requiring additional hardware.

The complexity of induction motors arises from their nonlinear characteristics, which, combined with uncertainties in rotor variables, often make it difficult to identify many motor parameters [20]. To address this, indirect estimation methods are employed, leveraging measurable quantities such as stator voltage, current, and rotor speed to infer these unknown parameters. By integrating these known values into a structured estimation framework, it becomes possible to iteratively refine and control additional motor parameters with greater accuracy.

In this study, a three-phase induction motor was tested using real-time data acquisition via the dSPACE DS1104 platform. Measured signals, including stator currents, rotor speed, and voltage, were utilized in a mathematical model in MATLAB/Simulink for parameter estimation. The identified parameters included stator resistance (R_s), rotor resistance (R_r), magnetizing inductance (L_m), stator leakage inductance (L_s), rotor leakage inductance (L_r), moment of inertia (J_m), friction coefficient (f), and the number of pole pairs (p). The Parameter Estimator App iteratively refined these parameters by minimizing discrepancies between simulated and experimental results. This methodology ensures precise parameter identification, which is crucial for enhancing motor performance, optimizing energy efficiency, and improving operational reliability in industrial applications.

II. THREE-PHASE INDUCTION MACHINE MODEL

Modeling an asynchronous machine relies on mathematical equations derived from its physical principles. However, as the model becomes more accurate, its complexity increases, demanding significant computational power [21]. To create a realistic and manageable model, simplifying assumptions are applied. These assumptions filter out less significant effects while preserving key dynamic and static behaviors, ensuring the model is practical and efficient for analysis and control.

To develop an effective mathematical model of the asynchronous machine, the following simplifying assumptions are made:

- The machine is symmetrical, and the air gap remains constant current density is uniformly distributed across conductor sections.
- The magnetic circuit is considered unsaturated and perfectly laminated in both the stator and rotor.
- Winding resistances are assumed to be temperature-independent, with skin and notch effects neglected.
- The magneto motive force (MMF) distribution is sinusoidal along the air gap.
- The cage rotor is modeled as an equivalent balanced three-phase winding.

Under the simplifying assumptions and for a balanced machine, the equations of the machine are written as follows:

A. Electrical Equations

The voltage equations for the three stator phases and the three rotor phases in matrix form are given by:

$$\begin{bmatrix} v_{sa} \\ v_{sb} \\ v_{sc} \\ v_{ra} \\ v_{rb} \\ v_{rc} \end{bmatrix} = \begin{bmatrix} R_s & 0 & 0 & 0 & 0 & 0 \\ 0 & R_s & 0 & 0 & 0 & 0 \\ 0 & 0 & R_s & 0 & 0 & 0 \\ 0 & 0 & 0 & R_r & 0 & 0 \\ 0 & 0 & 0 & 0 & R_r & 0 \\ 0 & 0 & 0 & 0 & 0 & R_r \end{bmatrix} \begin{bmatrix} i_{sa} \\ i_{sb} \\ i_{sc} \\ i_{ra} \\ i_{rb} \\ i_{rc} \end{bmatrix} + \frac{d}{dt} \begin{bmatrix} \phi_{sa} \\ \phi_{sb} \\ \phi_{sc} \\ \phi_{ra} \\ \phi_{rb} \\ \phi_{rc} \end{bmatrix} \quad (1)$$

The voltage equation of a three-phase induction machine describes the relationship between the stator and rotor voltages, currents, resistances, and flux linkages. The stator phase voltages, denoted as v_{sa}, v_{sb}, v_{sc} represent the electrical potential applied to the stator windings, while the rotor phase voltages, v_{ra}, v_{rb}, v_{rc} correspond to the voltages induced in the rotor windings. These voltages are influenced by the stator and rotor resistances, represented by R_s and R_r, respectively.

The stator currents, i_{sa}, i_{sb}, i_{sc} flow through the stator windings and interact with the magnetic field to generate torque. Similarly, the rotor currents, i_{ra}, i_{rb}, i_{rc} circulate in the rotor windings and contribute to the electromechanical energy conversion process. These currents influence the stator and rotor flux linkages, which are represented by $\phi_{sa}, \phi_{sb}, \phi_{sc}$ for the stator and $\phi_{ra}, \phi_{rb}, \phi_{rc}$ for the rotor. The flux linkages play a crucial role in determining the machine's dynamic response and its ability to develop torque [22].

B. Magnetic equation

The magnetic equations describe the relationship between the stator and rotor flux linkages and the corresponding phase currents. Under the assumption of linear magnetic behavior, the flux linkages can be expressed as a function of self and mutual inductances. The stator flux linkages $\phi_{as}, \phi_{bs}, \phi_{cs}$ are related to the stator currents (i_{as}, i_{bs}, i_{cs}) and rotor currents (i_{ar}, i_{br}, i_{cr}) through the stator selfinductance matrix $[L_{ss}]$ and the mutual inductance matrix $[L_{sr}]$. Similarly, the rotor flux linkages $\phi_{ar}, \phi_{br}, \phi_{cr}$ depend on the rotor self-inductance matrix $[L_{rr}]$ and the mutual inductance matrix $[L_{sr}]$, which represents the coupling between the stator and rotor windings.

$$\begin{bmatrix}\varphi_{as}\\ \varphi_{bs}\\ \varphi_{cs}\end{bmatrix} = [L_{ss}]\begin{bmatrix}i_{as}\\ i_{bs}\\ i_{cs}\end{bmatrix} + [L_{sr}]\begin{bmatrix}i_{ar}\\ i_{br}\\ i_{cr}\end{bmatrix} \tag{2}$$

$$\begin{bmatrix}\varphi_{ar}\\ \varphi_{br}\\ \varphi_{cr}\end{bmatrix} = [L_{rr}]\begin{bmatrix}i_{ar}\\ i_{br}\\ i_{cr}\end{bmatrix} + [L_{sr}]\begin{bmatrix}i_{as}\\ i_{bs}\\ i_{cs}\end{bmatrix} \tag{3}$$

The self-inductance matrices for the stator and rotor are defined as:

$$[L_{ss}] = \begin{bmatrix}L_{as} & M_{as} & M_{as}\\ M_{as} & L_{as} & M_{as}\\ M_{as} & M_{as} & L_{as}\end{bmatrix},\ [L_{rr}] = \begin{bmatrix}L_{ar} & M_{ar} & M_{ar}\\ M_{ar} & L_{ar} & M_{ar}\\ M_{ar} & M_{ar} & L_{ar}\end{bmatrix} \tag{4}$$

where L_{as} and L_{ar} are the stator and rotor self-inductances, while M_{as} and M_{ar} are the mutual inductances between the stator and rotor windings, respectively The stator-rotor mutual inductance matrix $[L_{sr}]$ is given by:

$$[L_{sr}] = \begin{bmatrix}\cos(\theta) & \cos\left(\theta - \frac{2\pi}{3}\right) & \cos\left(\theta + \frac{2\pi}{3}\right)\\ \cos\left(\theta + \frac{2\pi}{3}\right) & \cos(\theta) & \cos\left(\theta - \frac{2\pi}{3}\right)\\ \cos\left(\theta - \frac{2\pi}{3}\right) & \cos\left(\theta + \frac{2\pi}{3}\right) & \cos(\theta)\end{bmatrix} \tag{5}$$

Finally, the three-phase asynchronous machine model is expressed as:

$$\begin{cases}[v_{sabc}] = [R_s]\cdot[i_{sabc}] + \frac{d}{dt}([L_s]\cdot[i_{sabc}] + [L_{sr}]\cdot[i_{rabc}])\\ [v_{rabc}] = [R_r]\cdot[i_{rabc}] + \frac{d}{dt}([L_r]\cdot[i_{rabc}] + [L_{rs}]\cdot[i_{sabc}])\end{cases} \tag{6}$$

where $[v_{sabc}]$ and $[v_{rabc}]$ represent the stator and rotor voltage vectors, $[R_s]$ and $[R_r]$ are the stator and rotor resistance matrices, and $[i_{sabc}]$ and $[i_{rabc}]$ are the current vectors.

C. Mechanical equation

The electromagnetic torque equation for a three-phase induction machine in the d, q rotating reference frame is given by:

$$C_e = \frac{3}{2}pL_m\left(I_{qs}I_{dr} - I_{ds}I_{qr}\right) \tag{7}$$

where: C_e is Electromagnetic torque (Nm),p is Number of pole pairs,L_m is mutual inductance between stator and rotor (H),I_{qs} and I_{ds} is stator q-axis and d-axis currents (A),I_{dr} and I_{qr} is Rotor d-axis and q-axis currents (A).

III. SIMULATION OF INDUCTION MACHINE DYNAMICS

The simulation of an induction machine begins with transforming the three-phase electrical system into a decoupled two-phase (d-q) reference frame using Park's transformation [23]. This simplifies the complex three-phase differential equations into a set of equations that separate the direct-axis (d) and quadrature-axis (q) components decoupling flux and torque dynamics. The transformation enables the use of state-space representation, which is essential for efficient numerical computation and real-time simulation of both electrical and mechanical behavior [24].

The state-space form represents a dynamic system using a set of first-order differential equations:

$$\begin{aligned}\dot{x} &= Ax + BU + EC_r\\ y &= Cx\end{aligned} \tag{8}$$

- State Vector (x)

The system states are typically chosen as:

$$x = \begin{bmatrix} I_{ds} \\ I_{qs} \\ I_{dr} \\ I_{qr} \\ \omega \end{bmatrix} \tag{9}$$

Where: ω is rotor angular speed.
The control inputs applied to the system are the stator voltages:

$$U = \begin{bmatrix} V_{ds} \\ V_{qs} \end{bmatrix} \tag{10}$$

Where V_{sd}, V_{sq} are the $d-q$ components of stator voltage.

- Output Equation ($y = Cx$)

The measured system outputs are typically the stator currents:

$$y = \begin{bmatrix} I_{ds} \\ I_{qs} \end{bmatrix} \tag{11}$$

Where C is the output matrix:

$$C = \begin{bmatrix} 1 & 0 & 0 & 0 & 0 \\ 0 & 1 & 0 & 0 & 0 \end{bmatrix} \tag{12}$$

- Rotor Speed Dynamics

The rotor dynamics are governed by:

$$\frac{d\omega}{dt} = \frac{C_e P}{f} - \frac{C_r P}{f} - \frac{f}{J}\omega \tag{13}$$

Where C_r is Load torque,P is number of pole pairs,f is friction coefficient and J is rotor inertia. Substituting Eq. (7) into Eq. (13), the speed equation becomes:

$$\frac{d\omega}{dt} = \sigma P J I_{qs} I_{dr} - \sigma P J I_{ds} I_{qr} - C_r \frac{P}{J} b\omega \tag{14}$$

Where σ gave as $\sigma = \frac{3}{2} P L_m$

- System Matrices

The state matrix A describes how the system states evolve:

$$A = \begin{bmatrix} -\frac{1}{T_s \sigma} & \omega_s + (1/\sigma - 1)\omega & -\frac{M}{L_s T_r \sigma} & -\frac{M}{L_s \sigma}\omega & 0 \\ -\left(\omega_s + \frac{(1-\sigma)\omega}{\sigma}\right) & -\frac{1}{T_s \sigma} & -\frac{M}{L_s \sigma}\omega & -\frac{M}{L_s T_r \sigma} & 0 \\ \frac{M}{L_r T_s \sigma} & -\frac{M}{L_r \sigma}\omega & -\frac{1}{T_r \sigma} & \omega_s - \left(1 - \frac{M^2}{L_s L_r \sigma}\right)\omega & 0 \\ \frac{M}{L_r \sigma}\omega & \frac{M}{L_r T_s \sigma} & -\omega_s + \left(1 - \frac{M^2}{L_s L_r \sigma}\right)\omega & -\frac{1}{T_r \sigma} & 0 \\ 0 & \frac{\sigma p}{J} I_{dr} & 0 & -\frac{\sigma p}{J} I_{ds} & -\frac{f}{J} \end{bmatrix} \tag{15}$$

The input matrix B defines how the control inputs, specifically the stator voltages V_{ds} and V_{qs}, influence the state variables, particularly the stator currents I_{ds} and I_{qs}, while the rotor flux components and rotor speed remain indirectly affected through system dynamics. It is given by:

$$B = \begin{bmatrix} \frac{1}{L_s} & 0 \\ 0 & \frac{1}{L_s} \\ 0 & 0 \\ 0 & 0 \\ 0 & 0 \end{bmatrix} \tag{16}$$

Similarly, the disturbance matrix E accounts for external disturbances such as the load torque C_r, primarily affecting the rotor speed dynamics, and is expressed as:

$$E = \begin{bmatrix} 0 \\ 0 \\ 0 \\ 0 \\ \frac{P}{J} \end{bmatrix} \tag{17}$$

The block diagram in Figure 1 illustrates the comprehensive simulation framework for an induction machine, highlighting the integration of various components. The simulation begins with time-based inputs for stator voltages Vds and Vqs, which are fed into the system as experimental data. Additionally, the synchronous speed (ws) is calculated using 2×p×π/50, where p is the number of pole pairs. The load torque (Cr) is initially set to zero but can be adjusted to simulate different loading conditions. These inputs are processed through the induction motor model, which calculates the corresponding currents Ids and Iqs, as well as the rotor speed w.

The middle section of the block diagram focuses on the state-spac representation of the induction machine dynamics. The state-space matrices A(x), B, and E describe the evolution of the system states over time. The state vector x includes variables such as stator currents, rotor fluxes, and rotor speed, which are updated at each time step based on the input voltages and load torque. The derivative of the state vector (dx/dt) is calculated using the state matrix A(x) and the input matrix B. This derivative is then integrated to update the state vector for the next time step. The calculated stator currents (Ids, Iqs), rotor fluxes (ψrd, ψrq), and rotor speed (w) are outputted from this section.

In the bottom section, the state matrix A(x) is decomposed into five sub-matrices (A1, A2, A3, A4, A5) to account for dependencies on angular speeds (ωs, ω), rotor flux (φrd), and stator current (Ids). Each sub-matrix captures specific aspects of the induction machine dynamics. For example, A1 captures basic resistive and inductive effects, A2 accounts for the influence of synchronous speed (ωs), A3 considers the impact of rotor speed (ω), and A4 and A5 incorporate the effects of rotor flux (φrd) and stator current (Ids), respectively. contributions from all sub-matrices are combined to form the complete state matrix A(x), which is used to update the state vector. The matrix A defined as follows:

$$\mathbf{A} = \boldsymbol{A_1} + \boldsymbol{A_2\omega_s} + \boldsymbol{A_3\omega} + \boldsymbol{A_4 I_{dr}} + \boldsymbol{A_5 I_{ds}} \tag{18}$$

Matrix $\boldsymbol{A_1}$:

$$\boldsymbol{A_1} = \begin{bmatrix} \frac{1}{T_s\sigma} & 0 & \frac{M}{L_s T_s} & 0 & 0 & 0 \\ 0 & \frac{1}{T_s\sigma} & 0 & \frac{M}{L_s T_s} & 0 & 0 \\ 0 & 0 & -\frac{1}{T_s\sigma} & 0 & \frac{M}{L_s T_s \sigma} & 0 \\ 0 & 0 & 0 & -\frac{1}{T_r\sigma} & 0 & \frac{M}{L_r T_r \sigma} \\ 0 & 0 & 0 & 0 & 0 & 1 \\ 0 & 0 & 0 & 0 & -\frac{p}{J} & -\frac{f}{J} \end{bmatrix} \tag{19}$$

Matrix $\boldsymbol{A_2}$:

$$\boldsymbol{A_2} = \begin{bmatrix} 0 & -1 & 0 & 0 & 0 & 0 \\ 1 & 0 & 0 & 0 & 0 & 0 \\ 0 & 0 & 0 & -1 & 0 & 0 \\ 0 & 0 & 1 & 0 & 0 & 0 \\ 0 & 0 & 0 & 0 & 0 & 1 \\ 0 & 0 & 0 & 0 & -1 & 0 \end{bmatrix} \tag{20}$$

Matrix $\boldsymbol{A_3}$:

$$\boldsymbol{A_3} = \begin{bmatrix} 0 & 1 & 0 & \frac{M}{L_{s''}} & 0 & 0 \\ -1 & 0 & -\frac{M}{L_{s''}} & 0 & 0 & 0 \\ 0 & \frac{M}{L_{s''}} & 0 & -\left(\frac{M^2}{L_{s'} L_{r''}} + 1\right) & 0 & 0 \\ -\frac{M}{L_{s''}} & 0 & \frac{M^2}{L_s L_{r''}} + 1 & 0 & 0 & 0 \\ 0 & 0 & 0 & 0 & 0 & 1 \\ 0 & 0 & 0 & 0 & -1 & 0 \end{bmatrix} \tag{21}$$

Matrix $\boldsymbol{A_4}$:

$$\boldsymbol{A_4} = \begin{bmatrix} 0 & 0 & 0 & 0 & 0 & 0 \\ 0 & 0 & 0 & 0 & 0 & 0 \\ 0 & 0 & 0 & 0 & 0 & 0 \\ 0 & 0 & 0 & 0 & 0 & 0 \\ 0 & 0 & 0 & 0 & 0 & 0 \\ \frac{\alpha P}{\delta} & 0 & 0 & 0 & 0 & 0 \end{bmatrix} \tag{22}$$

Matrix $\boldsymbol{A_5}$:

$$\boldsymbol{A_5} = \begin{bmatrix} 0 & 0 & 0 & 0 & 0 & 0 \\ 0 & 0 & 0 & 0 & 0 & 0 \\ 0 & 0 & 0 & 0 & 0 & 0 \\ 0 & 0 & 0 & 0 & 0 & 0 \\ 0 & 0 & 0 & 0 & 0 & 0 \\ 0 & -\frac{\alpha P}{\delta} & 0 & 0 & 0 & 0 \end{bmatrix} \tag{23}$$

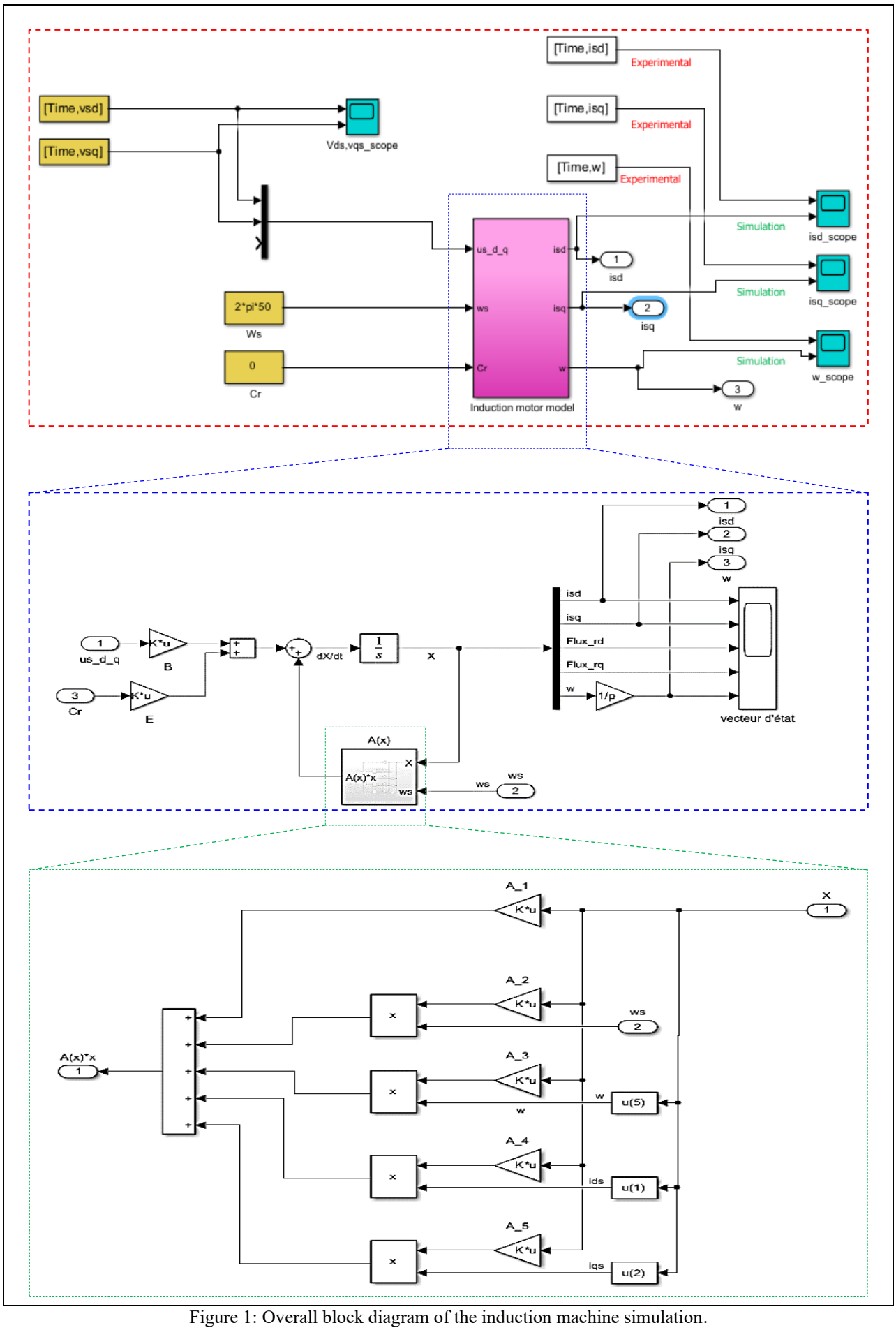

Figure 1: Overall block diagram of the induction machine simulation.
Source: Authors, (2025).

IV. METHODOLOGY FOR EXPERIMENTAL TESTS

IV. I. IMPORTING EXPERIMENTAL DATA

The first step in identifying the parameters of the induction motor is to collect experimental data by measuring the stator currents (I_{ds}, I_{qs}) and rotor speed (ω), which serve as key signals for modeling the system's dynamics. The block diagram in Figure 2 illustrates the hardware setup for the induction motor, which utilizes a dSPACE DS1104 interface board. The setup consists of the following key components:

- Three-Phase Network (50 Hz): Provides the AC power supply to the system.
- Auto Transformer: Regulates the voltage supplied to the induction motor, ensuring controlled variations in input voltage for identification purposes.
- Three-Phase Switch: Enables controlled connection and disconnection of the motor, allowing transient excitation to capture dynamic response data.
- Voltage and Current Sensors (abc): Measure the three-phase stator voltages (Va,Vb,Vc) and currents (Ia,Ib,Ic) for conversion into the dq-axis reference frame.
- Induction Motor: The system under test, whose electrical and mechanical characteristics are identified through measured responses.
- Incremental Encoder: Measures the rotor speed (ω) by providing real-time position feedback, which is converted into speed signals.
- Control Desk with dSPACE DS1104: Processes and records real-time data, saving results as .m files for further analysis in MATLAB.

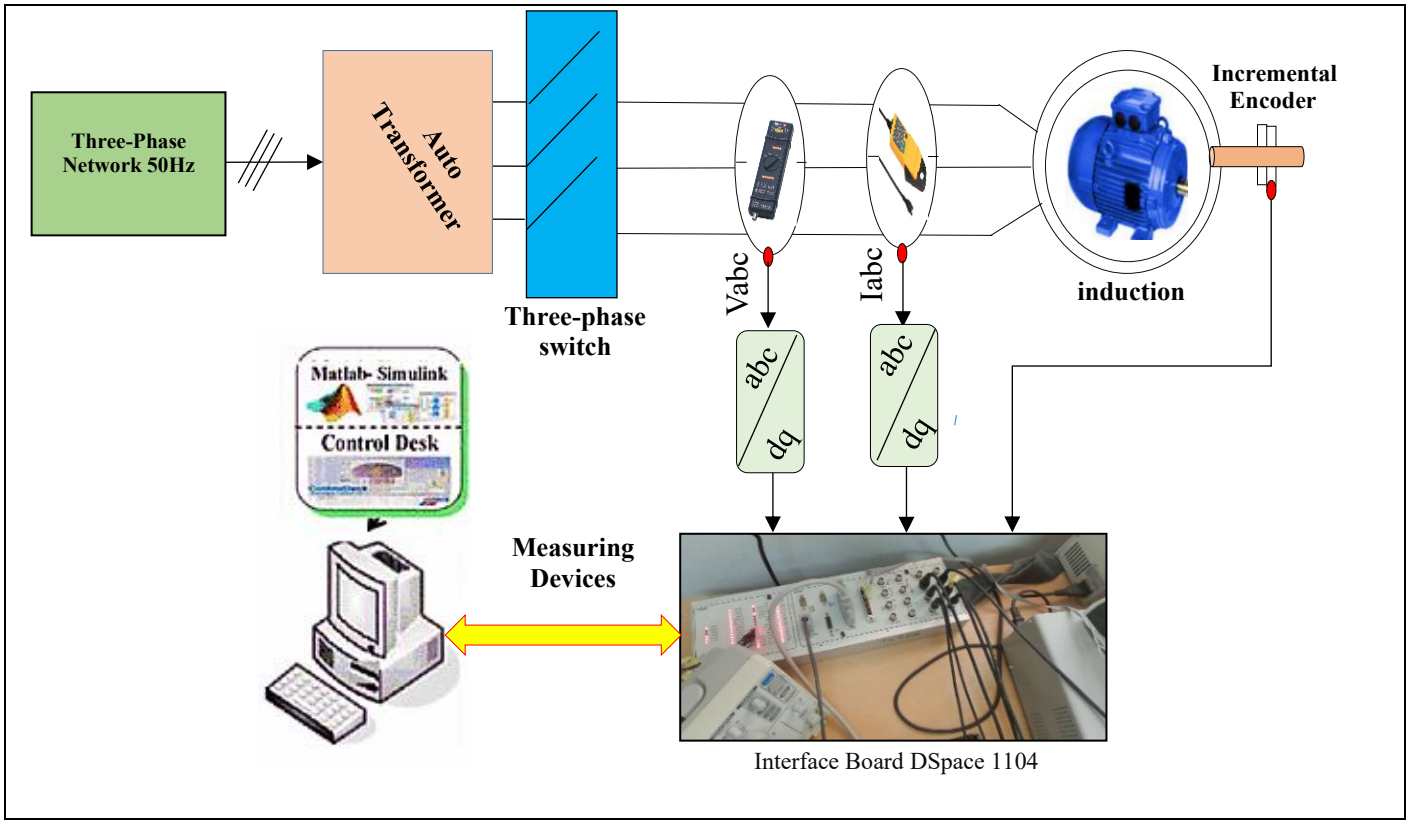

Figure 2: Overall block diagram of the experimental setup.
Source: Authors, (2025).

The Siemens induction motor, whose nameplate details are provided in Appendix A, is powered by a three-phase 50 Hz network with an auto-transformer to regulate the supply voltage. A three-phase switch is introduced to create controlled transient conditions, enabling the measurement of system responses under both steady-state and dynamic conditions.The stator currents (I_a, I_b, I_c) and voltages (V_a, V_b, V_c) are measured using sensors and then transformed into dq-axis components via an abc/dq transformation, allowing analysis in a synchronous reference frame. The rotor speed (ω) is recorded using an incremental encoder, providing real-time speed signals for accurate evaluation.These signals are processed by the dSPACE DS1104 interface board, which digitizes and transmits the data to MATLAB/Simulink ControlDesk for real-time monitoring and logging, as illustrated in Figure 3. This collected data is crucial for identifying motor parameters and characterizing its behavior under various operating conditions.

After importing the experimental data, open the simulation model, which includes the induction motor, as shown in Figure 1. To ensure accurate analysis, the experimental data, including rotor speed (ω), stator currents (I_{ds}, I_{qs}), and voltages (V_{ds}, V_{qs}), as presented in Figure 4, must be entered into the simulation. Before execution, the .m file available in Appendix B, which contains the motor's installed

parameters, must be loaded to initialize the system correctly. This step ensures precise parameter identification and validation by comparing the dynamic responses of simulated and experimental results, as illustrated in Figures 5,6 and 7 for I_{ds}, I_{qs}, and ω, respectively.

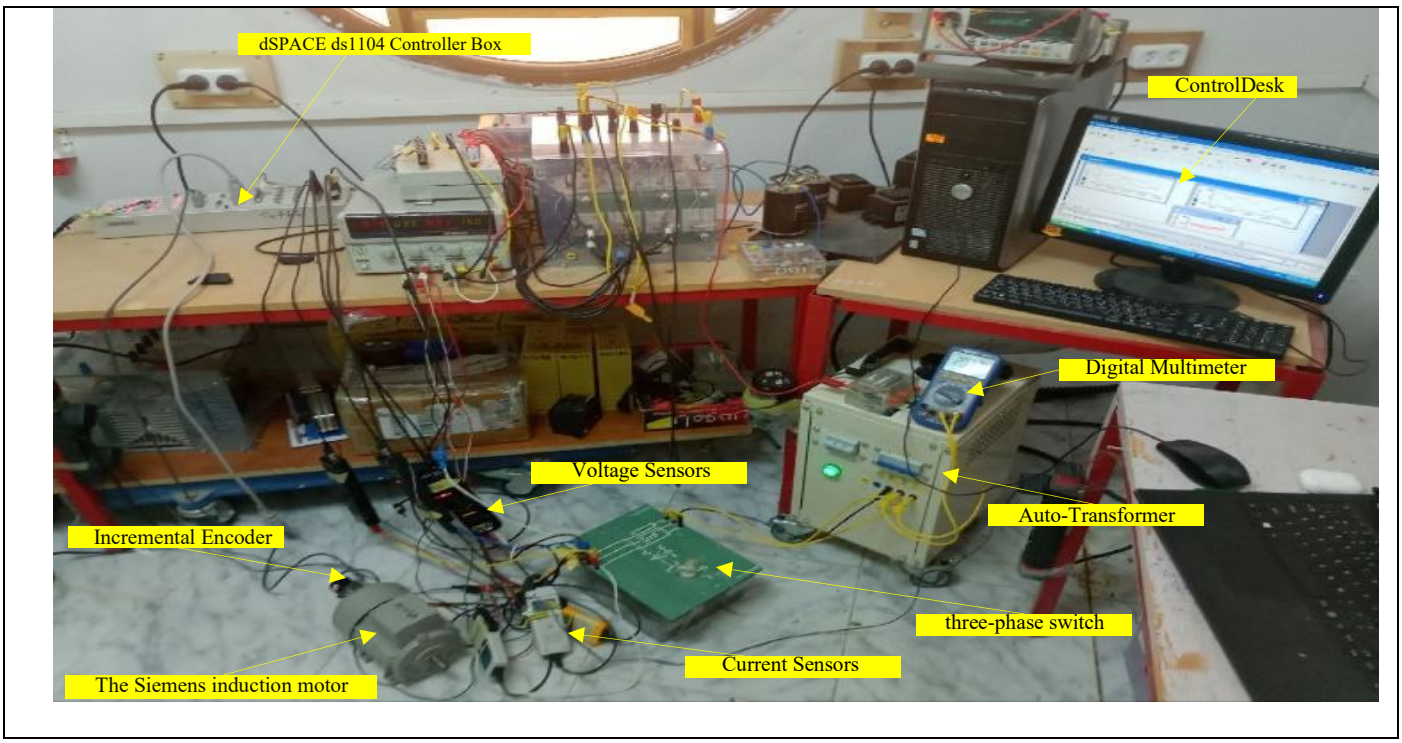

Figure 3: Overall block diagram of the experimental setup.
Source: Authors, (2025).

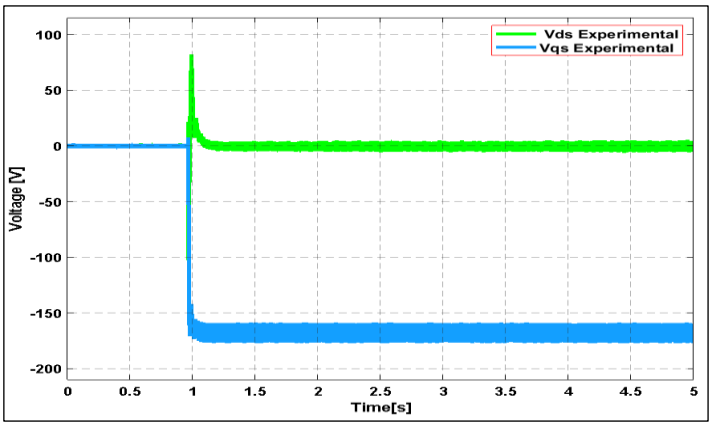

Figure 4: Experimental Responses of Vds and Vqs Voltage.
Source: Authors, (2025).

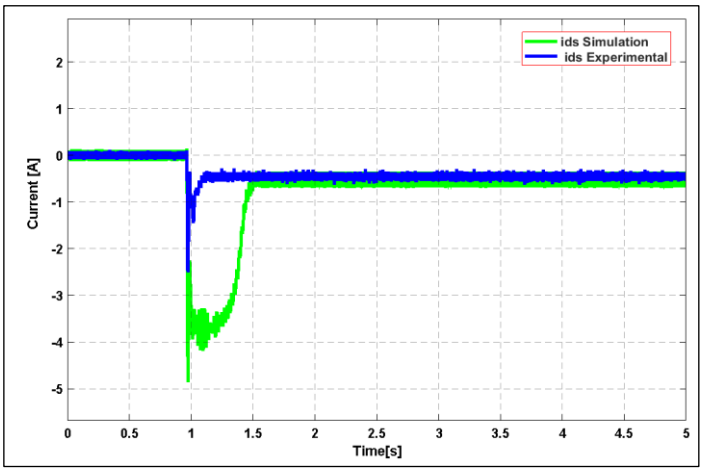

Figure 5: Dynamic Responses of Simulated and Experimental ids.
Source: Authors, (2025).

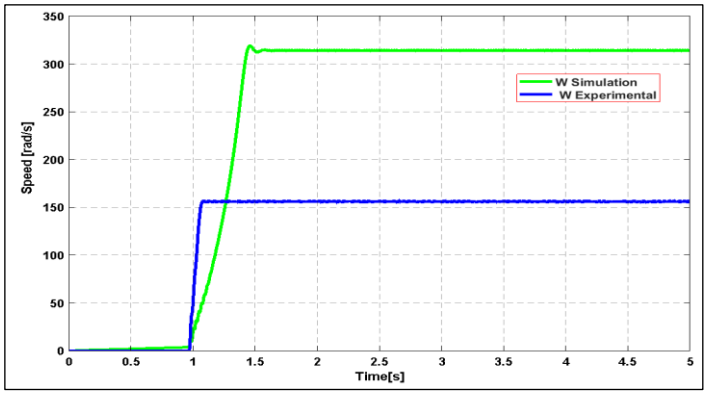

Figure 6: Dynamic Responses of Simulated and Experimental iqs.
Source: Authors, (2025).

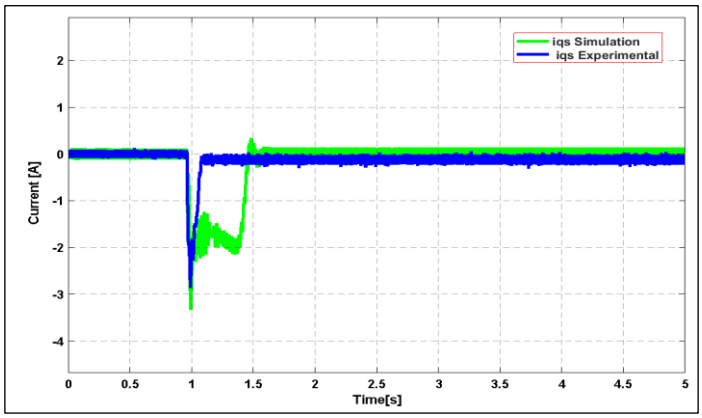

Figure 7: Dynamic Responses of Simulated and Experimental W.
Source: Authors, (2025).

IV.2 PARAMETER ESTIMATION PROCESS

To estimate the parameters of the induction motor using MATLAB's Parameter Estimator app, follow these steps:

The first step is to launch the Parameter Estimator. This can be done from the Simulink induction motor model by navigating to the Apps tab. Under Control Systems, click Parameter Estimator. Doing so will open the Parameter Estimation tool, which provides a user-friendly interface for configuring and executing the parameter estimation process. Alternatively, the tool can also be launched directly from the MATLAB command prompt by entering the command spetool('modelname'), where the model name is the name of the Simulink model. This command will open the Parameter Estimation tool for the specified model, allowing users to configure and run the estimation process efficiently.

Next, the measured experimental data must be imported for estimation. The required data consists of vds, vqs, ids, iqs, W, and Time, as shown in Figure 8. These values should be obtained from real-time measurements and saved in MAT files using ControlDesk. The Parameter Estimator also allows users to import data from other sources, such as MATLAB variables, Excel files, or comma-separated value (CSV) files, making it flexible for different applications.

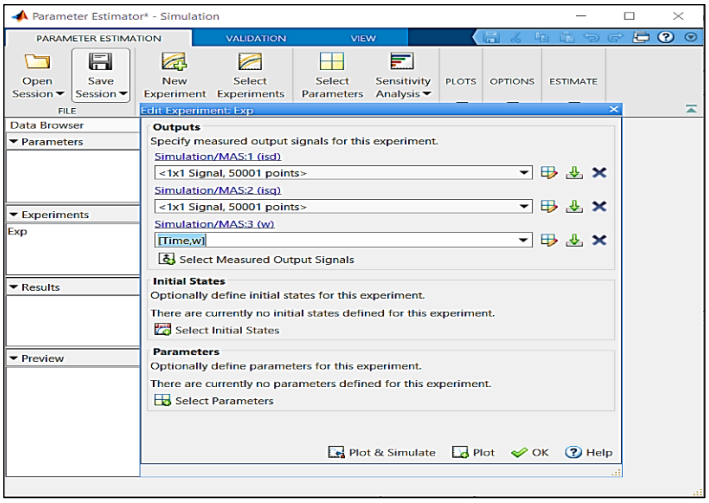

Figure 8: Selecting measured output signals in Parameter Estimator.
Source: Authors, (2025).

After importing the experimental data, the user must select the relevant experiment for inclusion in the estimation or validation process. The Parameter Estimator provides a dedicated interface for this selection, as shown in Figure 9. Choosing the appropriate experiments ensures that the estimation algorithm processes the correct dataset. Once the selection is finalized, clicking "OK" confirms the dataset for estimation, allowing the process to proceed efficiently.

Once the data has been successfully imported, the next step is to configure the induction motor parameters for estimation. The Parameter Estimator comes pre-loaded with key parameters relevant to the induction motor subsystem, including stator resistance (Rs), rotor resistance (Rr), magnetizing inductance (Lm), stator leakage inductance (Ls), rotor leakage inductance (Lr), moment of inertia (Jm), friction coefficient (f), and number of pole pairs (p). These parameters define the motor's electrical and mechanical behavior and are essential for accurate estimation.

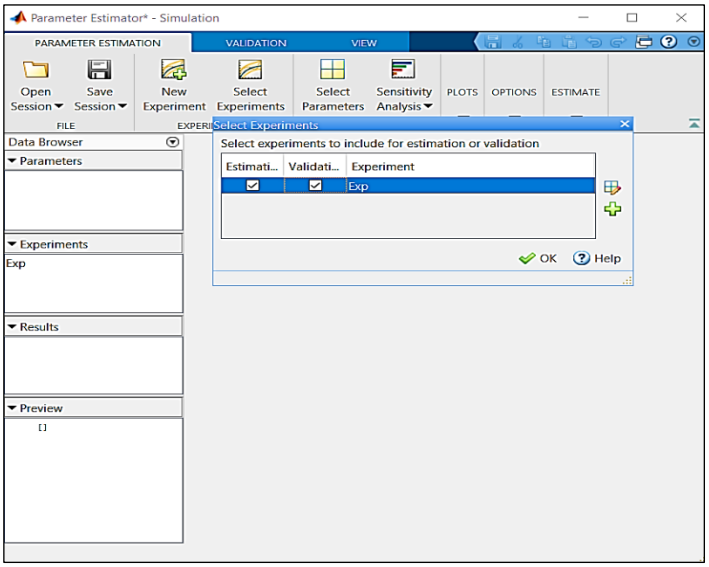

Figure 9: Selecting experiments for estimation and validation.
Source: Authors, (2025).

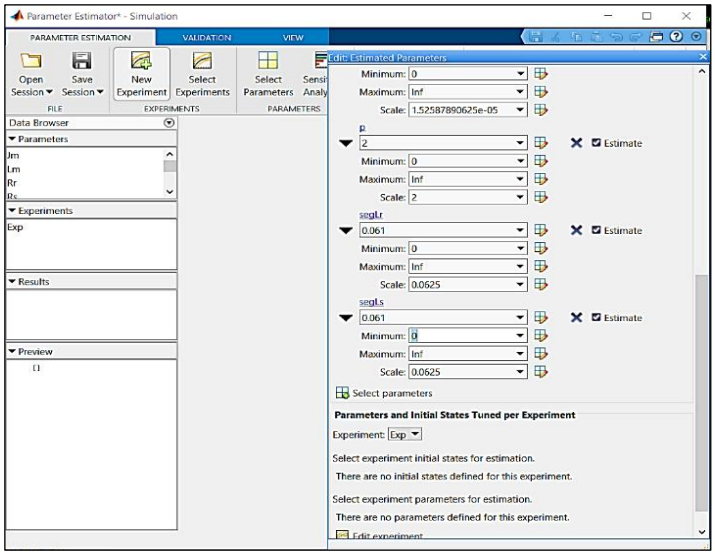

Figure 10: Parameter Selection and Constraint Configuration.
Source: Authors, (2025).

After defining the parameters, it is necessary to set appropriate constraints to ensure physically meaningful results. Each parameter should be confined within a realistic range, typically from 0 to a positive upper bound, preventing the estimation of non-physical negative values. This step is crucial for achieving reliable and valid results, as shown in Figure 10.

With all configurations set, the next step is to initiate the parameter estimation process. Clicking the "Run" button starts the optimization, where the Parameter Estimator iteratively adjusts the parameter values to minimize the error between simulated and measured responses, as shown in Figure 11. The estimation app continuously refines the parameters to achieve the best possible match with the experimental data, ensuring accuracy and reliability in the model.

Finally, once the estimation is complete, the estimated parameters must be validated. The user should compare the simulated motor response with the measured data to ensure a close fit. If discrepancies arise, adjustments to the parameter constraints or dataset may be necessary, followed by rerunning the estimation process. Through iterative refinement, the accuracy of the identified parameters can be significantly enhanced, leading to a more reliable and precise model.

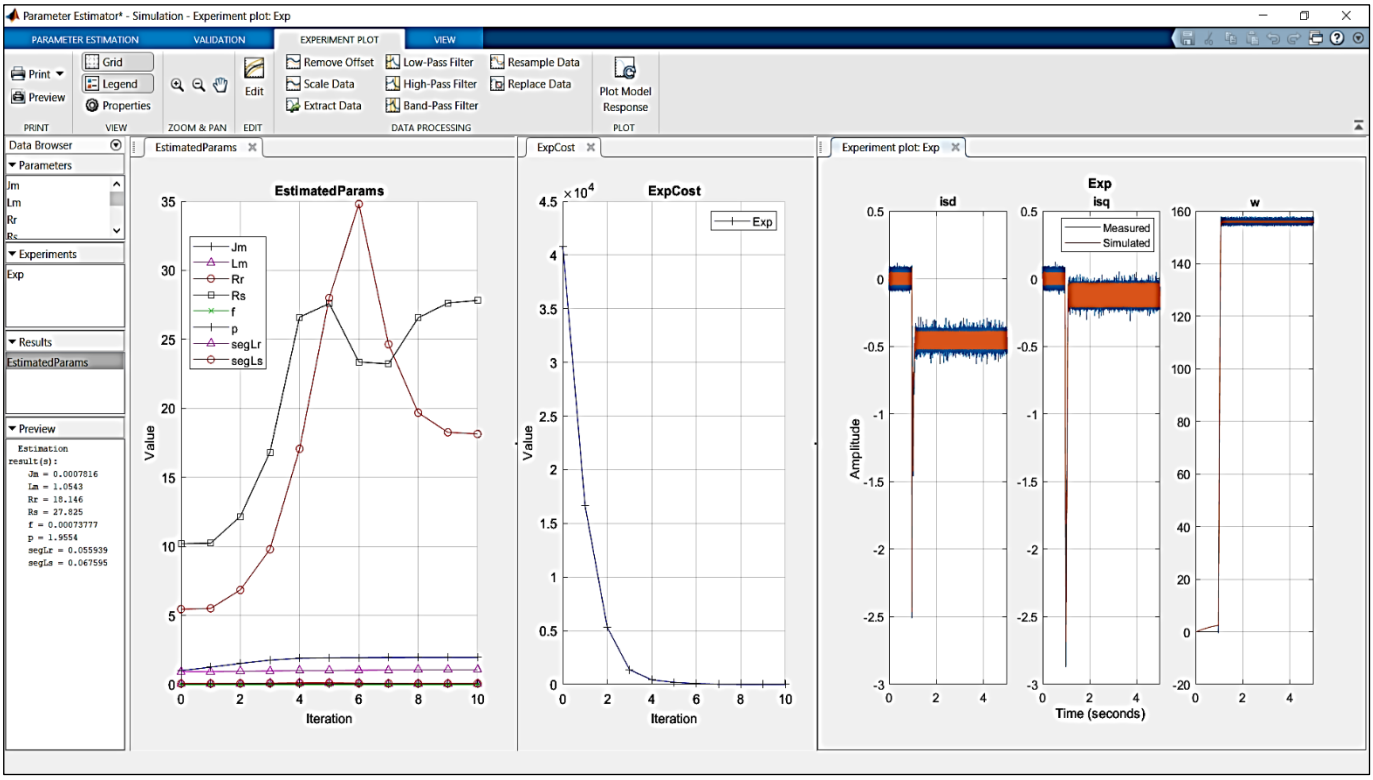

Figure 11: Convergence of Estimated Parameters and Error Minimization in MATLAB Parameter Estimator.
Source: Authors, (2025).

Appendix A

Siemens Induction Motor Nameplate. The corresponding nameplate is shown in Figure A1. This information is essential for identifying the motor's operating parameters and ensuring proper integration into the system.

Figure 1: Siemens induction motor nameplate.
Source: Authors, (2025).

Appendix B

Motor Parameter Initialization File

The following MATLAB script initializes the parameters of the three-phase induction motor. It defines the motor's electrical and mechanical parameters, ensuring accurate simulation and analysis. The script also loads experimental data from mesures.mat, which includes time, rotor speed (W), stator currents (i_{sd}, i_{sq}), and voltages (v_{sd}, v_{sq}).

```
clear;
clc;
%--------- Initial Parameters ---------
Rs = 10.2; % Stator resistance (measured directly using an ohmmeter)
Rr = 5.45; % Rotor resistance
Lm = 0.921; % Mutual inductance
% Ensure Ls and Lr > Lm using: Ls = segLs + Lm, Lr = segLr + Lm
segLs = 0.061; % Stator leakage inductance
```

```
segLr = 0.061; % Rotor leakage inductance
Jm = 0.00095; % Moment of inertia
f = 0.00001; % Friction coefficient
p = 1;     % Number of pole pairs
% Load experimental data
load('mesures.mat');
Time = mesures.X.Data';
w = mesures.Y(1).Data';
isd = mesures.Y(2).Data';
isq = mesures.Y(3).Data';
vsd = mesures.Y(4).Data';
vsq = mesures.Y(5).Data';
```

VI. CONCLUSIONS

In This study presents a methodology for estimating the parameters of a three-phase induction motor by integrating experi-mental data with simulation. Real-time data, including stator currents, rotor speed, and voltage signals, were collected through an experimental setup utilizing the dSPACE DS1104 platform. This dataset was then applied to a mathematical model of the motor in MATLAB/Simulink, representing its dynamic behavior with approximate initial pa-rameters. The Parameter Estimator App was then used to refine these parameters by iteratively adjusting their values to minimize the error between the simulated and measured responses. By initiating the estimation process, the app continu-ously optimized the parameters to achieve the best possible match with the experimental data, ensuring accuracy and relia-bility. The validation was performed using a Siemens 0.37 kW, 50 Hz, 380 V three-phase induction motor operating under zero-load conditions, where the cost function reached near zero, indicating a strong agreement between the simulated and experimental results. This approach ensures precise parameter identification, which is essential for control and diagnostic applications, with potential future extensions to other motor types for broader industrial applications.

VI. AUTHOR'S CONTRIBUTION

Conceptualization: Fares Bettahar, Sabrina Abdeddaim and Achour Betka, Michael Short and Maher Al-Greer
ethodology: Fares Bettahar and Sabrina Abdeddaim.
Investigation: Fares Bettahar and Sabrina Abdeddaim.
Discussion of results: Sabrina Abdeddaim and Achour Betka Laid Guerrida
Writing – Original Draft: Fares Bettahar.
Writing – Review and Editing: Fares Bettahar and Sabrina Abdeddaim .Belahcene taha lemdjed
Resources: Sabrina Abdeddaim.Omar Charrouf
Supervision: Sabrina Abdeddaim and Achour Betka.
Approval of the final text: Fares Bettahar, Sabrina Abdeddaim Achour Betka and Maher Al-Greer

VII. REFERENCES

[1] Dineva, A.; Mosavi, A.; Faizollahzadeh Ardabili, S.; Vajda, I.; Shamshirband, S.; Rabczuk, T.; Chau, K.-W. Review of Soft Computing Models in Design and Control of Rotating Electrical Machines. Energies 2019, 12(6), 1049. Available online: https://doi.org/10.3390/en12061049

[2] Merizalde, Y.; Hernández-Callejo, L.; Duque-Perez, O. State of the Art and Trends in the Monitoring, Detection and Diagnosis of Failures in Electric Induction Motors. Energies 2017, 10, 1056. Available online : https://doi.org/10.3390/en10071056

[3] Szénásy, I.; Csikor, D. Induction Motor Energy Efficiency Investigation. Engineering Proceedings 2024, 79(1), 75. Available online : https://doi.org/10.3390/engproc2024079075

[4] Liu, Z., Xu, L., & Xu, D. (2018). Advanced Control Strategies of Induction Machine: Field Oriented Control, Direct Torque Control, and Finite Set Model Predictive Control. Energies, 11(1), 120.

[5] Aktas, M.; Awaili, K.; Ehsani, M.; Arisoy, A. Direct torque control versus indirect field-oriented control of induction motors for electric vehicle applications. Engineering Science and Technology, an International Journal 2020, 23(5), 1134–1143. Available online: https://doi.org/10.1016/j.jestch.2020.04.002

[6] Bašić, M.; Vukadinović, D.; Grgić, I. Model Predictive Current Control of an Induction Motor Considering Iron Core Losses and Saturation. Processes 2023, 11(10), 2917. Available online : https://doi.org/10.3390/pr11102917

[7] Aktas, M.; Awaili, K.; Ehsani, M.; Arisoy, A. Direct torque control versus indirect field-oriented control of induction motors for electric vehicle applications. Engineering Science and Technology, an International Journal 2020, 23(5), 1134–1143. Available online: https://doi.org/10.1016/j.jestch.2020.04.002

[8] El Ouanjli, N.; Derouich, A.; El Ghzizal, A.; Motahhir, S.; Chebabhi, A.; El Mourabit, Y.; Taoussi, M. Modern improvement techniques of direct torque control for induction motor drives—a review. Protection and Control of Modern Power Systems 2019, 4(1), 11. Available online: https://doi.org/10.1186/s41601-019-0125-5

[9] Soliman, H.M. (2016). Effect of the Parameters Variation for Induction Motor on its Performance Characteristics with Field Oriented Control Compared to Scalar Control. International Journal of Engineering Research & Science (IJOER), 2(8), 1-7.

[10] Martin, C., Bermudez Guzman, M., Barrero, F., Arahal, M.R., Duran, M.J., & Kestelyn, X. (2017). Sensitivity of Predictive Controllers to Parameter Variation in Five-Phase Induction Motor Drives. Control Engineering Practice, 70, 1-12. https://sam.ensam.eu/handle/10985/13798

[11] Kačenka, A., Makys, P., & Struharnansky, L. (2020). Impact of Parameter Variation on Sensorless Indirect Field Oriented Control of Induction Machine. In I. Zelinka, P. Brandstetter, T. Trong Dao, V. Hoang Duy, & S. Kim (Eds.), AETA 2018 - Recent Advances in Electrical Engineering and Related Sciences: Theory and Application (pp. 799–809). Springer. https://doi.org/10.1007/978-3-030-14907-9_77

[12] Hanif, A., Ali, S. M. N., Ahmed, Q., Bhatti, A. I., & Aslam, M. (2016). Effect of Variation in Rotor Resistance on the Dynamic Performance of Induction Motor. In 2016 35th Chinese Control Conference (CCC) (pp. 5639–5644). IEEE. https://doi.org/10.1109/ChiCC.2016.7554869

[13] Harini, B. W. (2022). The Effect of Motor Parameters on the Induction Motor Speed Sensorless Control System using Luenberger Observer. International Journal of Applied Sciences and Smart Technologies, 4(1), 47–54. https://doi.org/10.24071/ijasst.v4i1.4518

[14] Kačenka, A., Makys, P., & Struharnansky, L. (2020). Impact of Parameter Variation on Sensorless Indirect Field Oriented Control of Induction Machine. In I. Zelinka, P. Brandstetter, T. Trong Dao, V. Hoang Duy, & S. Kim (Eds.), AETA 2018 - Recent Advances in Electrical Engineering and Related Sciences: Theory and Application (pp. 799–809). Springer. https://doi.org/10.1007/978-3-030-14907-9_77

[15] Et-taaj, L., Boulghasoul, Z., El Kharki, A., & Elbacha, A. (2022). Improvement of sensorless control of induction motor by voltage source inverter nonlinearities compensation and extended Kalman filter. Electrical Engineering, 104(6), 3509–3521. https://doi.org/10.1007/s00202-022-01560-1

[16] Tran, T. C., Brandstetter, P., Tran, C. D., Ho, S. D., Nguyen, M. C., & Phuong, P. N. (2019). Parameters Estimation for Sensorless Control of Induction Motor Drive Using Modify GA and CSA Algorithm. In AETA 2018 - Recent Advances in Electrical Engineering and Related Sciences: Theory and Application (pp. 580–591). Springer. https://doi.org/10.1007/978-3-030-14907-9_57

[17] Fagiano, L., Lauricella, M., Angelosante, D., & Ragaini, E. (2018). Identification of Induction Motors with Smart Circuit Breakers. arXiv preprint arXiv:1804.07817. https://arxiv.org/abs/1804.07817

[18] Susanto, J., & Islam, S. (2017). Improved Parameter Estimation Techniques for Induction Motors using Hybrid Algorithms. arXiv preprint arXiv:1704.02424. https://arxiv.org/abs/1704.02424

[19] Sarhan, H., Guimarães, J.M.C., Bernardes, J.V., Hermeto, A.E., & Bortoni, E.C. (2023). Numerical Estimation and Experimental Verification of Optimal Parameter Identification Based on Modern Optimization of a Three Phase Induction Motor. Mathematics, 7(12), 1135. https://doi.org/10.3390/math7121135

[20] Guo, H., Yang, X., Diao, N., Sun, X., Zhang, H., Zhao, X., Li, H., Hu, W., & Song, C. (2025). The least squares off-line parameter identification method of half-dead compensated induction motor based on non-π/3 angle virtual rotating vector orientation. Electrical Engineering, 107(1), 1–15. https://doi.org/10.1007/s00202-024-02893-9

[21] Belbali, A., Makhloufi, S., Kadri, A., Abdallah, L., & Seddik, Z. (2023). Mathematical Modeling of a Three-Phase Induction Motor. In Induction Motors-Recent Advances, New Perspectives and Applications. IntechOpen. https://doi.org/10.5772/intechopen.101358

[22] Le Roux, P. F., and M. K. Ngwenyama. 2022. "Static and Dynamic Simulation of an Induction Motor Using Matlab/Simulink" Energies 15, no. 10: 3564. https://doi.org/10.3390/en15103564

[23] Sengamalai, U.; Anbazhagan, G.; Thamizh Thentral, T.M.; Vishnuram, P.; Khurshaid, T.; Kamel, S. (2022). Three Phase Induction Motor Drive: A Systematic Review on Dynamic Modeling, Parameter Estimation, and Control Schemes.
Energies, 15(21), 8260. https://doi.org/10.3390/en15218260.

[24] M. Pucci, "State Space-Vector Model of Linear Induction Motors," in IEEE Transactions on Industry Applications, vol. 50, no. 1, pp. 195-207, Jan.-Feb. 2014, https://doi.org/10.1109/TIA.2013.2266351